Indian Geotechnical Journal, 37(4), 2007, 283-300

Effect of Dredging on Open Type Berthing Structure – A Numerical Study

K. Muthukkumaran[*] and R. Sundaravadivelu[**]

Introduction

Construction of piles and diaphragm wall supported berthing structure on marine soils undergo time dependant vertical and horizontal sub-soil displacement. Where the landside forms an approach to the berthing structure, the sub-soil displacement may generate axial and lateral loads on the piles and diaphragm wall. Additional lateral loading may also be caused due to earth pressure during land dredging (Figure 1). While the induced axial loading due to dredging is often minimized by placing a suitable coating on the piles and diaphragm wall, lateral loading from sub-soil displacement generated by dredging generally can not be avoided or reduced in this way. Sometimes the lateral loading may lead to structural distress or failure of the structures. Hence, the study of dredging effect on piles and diaphragm wall supported berthing structure is necessary.

The design of pile and diaphragm wall supported berthing structure subjected to lateral loading from horizontal soil movements may be based on semi-empirical or theoretical analysis. The literature on the adequacy of the finite element method (FEM) modeling of berthing structure to analyses their behaviour during dredging is limited. The available data are generally limited in extent and complicated by variations in geometry or soil conditions. Hence, there are many uncertainties in the estimation of bending moments and lateral deflections induced in piles and diaphragm wall under these conditions. If the bending moments and deflections induced in piles and diaphragm wall can be accurately estimated, then more cost effective construction procedures may be confidently implemented to take advantage of sizes and configurations of an alternative pile and diaphragm wall.

A full scale field test was performed to examine the lateral loading of pile and diaphragm wall from horizontal soil movement induced by dredging. This aspect was studied in detail during construction of a berthing structure at Jawaharlal Nehru Port Trust Mumbai, one of the major ports in India. When dredging work was undertaken, it was decided to monitor the lateral movements of berth, as the dredging depth increased. For this purpose, inclinometer tubes were installed in one of the diaphragm wall panels and another in one of the piles of the structure.

[*] Lecturer, Department of Civil Engineering, National Institute of Technology, Tiruchirappali -620 015, India. Email: kmk@nitt.edu

[**] Professor & Head, Department of Ocean Engineering, Indian Institute of Technology Madras, Chennai-600036, India. Email: rsun@iitm.ac.in

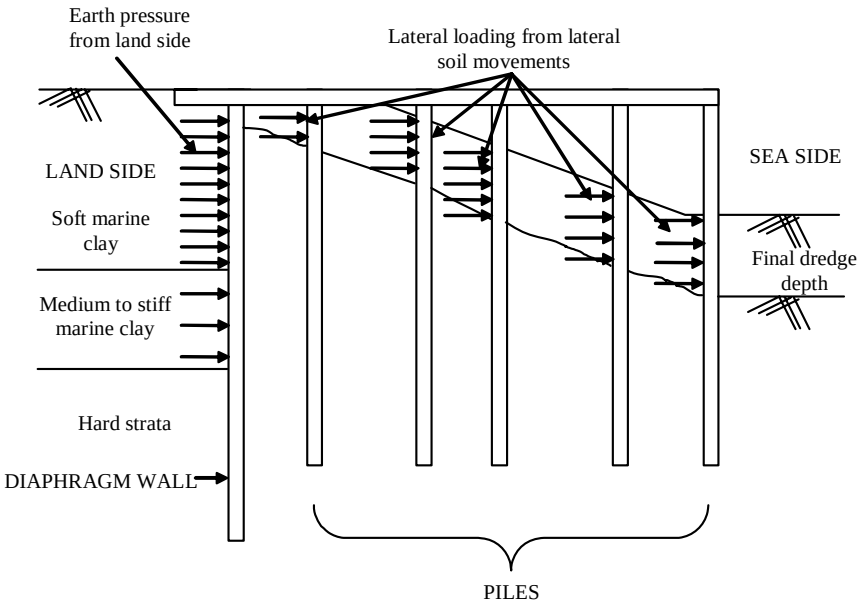

Fig. 1 Lateral Load from Land Side Generated by Dredging

The magnitude of the soil movement is related to many factors such as soil properties, structural properties and dredging sequence. A number of case histories have been reported in the literature which gives the relationship between those factors and wall deflection. Among these are Dibiagio and Myrvoll (1972), Davies (1982), Tedd et al. (1984), Clough and Rourke (1990) and Tamano et al. (1996). The aspects of their studies included the effects of wall construction on ground movements and changes in lateral earth and water pressure and numerical modeling of the effects of wall construction and ground movements. For Singapore soil conditions, Chen and Yap (1991) have reported the effects of the construction of diaphragm wall panel on the performance of the adjacent old masonry building associated. Poh et al. (2001) have reported the effect of diaphragm wall construction in Singapore soil condition. However, the field data available for the lateral ground movement induced by dredging is limited.

In this paper, a finite element approach is described for the analysis of piles and diaphragm wall supported berthing structure influenced by lateral soil movements generated by dredging. The approach is based on a plane strain representation of the problem. Results are compared with full scale field test results.

Details of Berthing Structure

Typical cross section of the berthing structure is shown in Figure2. The total length of the berth is 252m and width is 33m. The berth is supported by 1100 mm thick diaphragm wall and 5 rows of 1400mm diameter piles. The

diaphragm wall is terminated at a depth of -25.625m and the piles are terminated at a depth of -22.0m level. The natural ground level is +0.0m. To satisfy the berthing facility of the vessel the ground level is required to be dredged up to -9.5 m level. After completion of the structure when dredging work was undertaken, it was decided to monitor the behaviour of the berth, particular in the lateral deflection, as the dredge depth increased. The lateral deflection measurements were taken by using an inclinometer. The inclinometer readings were taken when the water depth in front of the structure was -3.0 m (without dredging) and -9.5 m (after –9.5 dredging). Two readings were taken at-9.5 m level, one immediately after reaching -9.5 m dredge level and another 3 months after completion of -9.5 m level dredge.

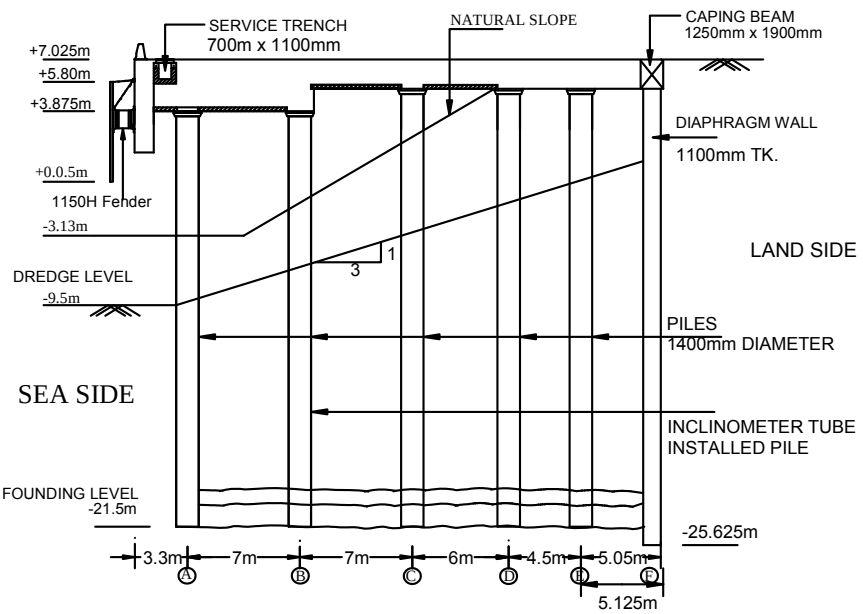

Section A-A

Fig. 2 Typical Cross Section of Berth

Geotechnical Data

Standard penetration test (SPT) was carried out in the site at several locations to understand the stratigraphy of the study area. Representative undisturbed and disturbed soil samples were collected for the laboratory test. Direct shear test, triaxial tests and unconfined compressive tests were performed. The design parameters of the soil obtained from the tests are presented in Table-1. A typical borehole detail is shown in Figure 3. The soil strata upto a depth of 6.0m from ground level is soft marine silty clay with undrained shear strength 20kN/m^2. This strata is followed by 2m medium stiff clay with undrained shear strength of 50kN/m^2. Below 15m level, the soil strata consists of hard marine silty clay which is followed by basalt rock. The actual

dredge level of -9.5m fall in the soft marine silty clay and medium stiff clay layers of low shear strength. During dredging, these soft strata may not be stable and may create stability problems to the existing structure, due to lateral movement of the structure in the unstable slope.

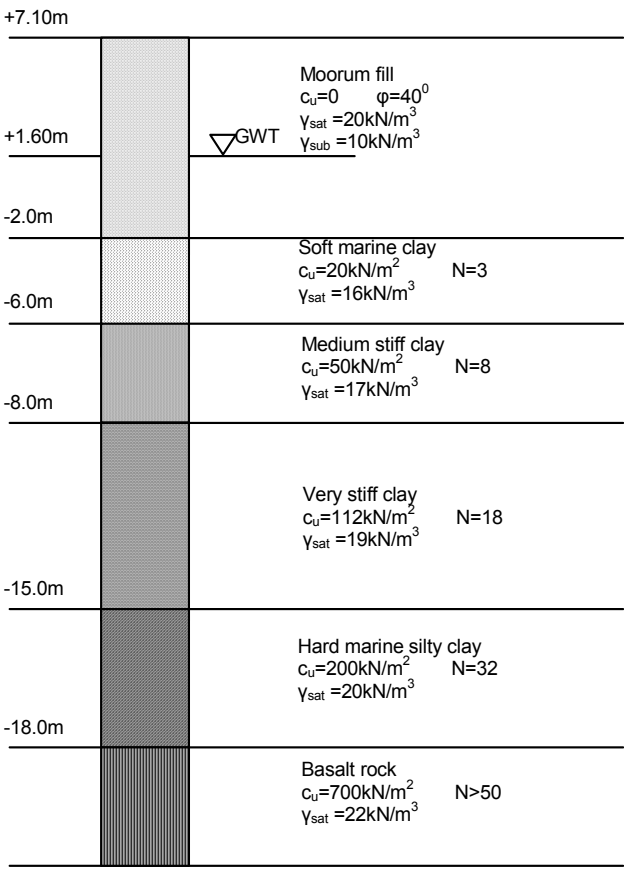

Fig. 3 Typical Borehole Details

Installation of Inclinometer Tube

The inclinometer tube made up of PVC is very flexible and can easily deform along with the deformation in the diaphragm wall and pile. During casting of diaphragm wall panel and pile, the inclinometer tube was placed with reinforcement cage. The location of inclinometer tube was chosen such that it was away from the tremie pipe location. The length of inclinometer tube above cut off level was closed and protected by rubber hose of 150 mm diameter. The annular gap between the rubber hose and inclinometer tube was filled with bentonite mud to ensure that no concrete enters the hose pipe during concreting.

Table 1: Soil Properties

Description	Density (γ_{sat}) (kN/m^3)	Untrained Shear Strength (kN/m^2)	Angle of Internal Friction (φ) (degree)	Angle of Dilatancy (ψ) (degree)	Young's Modulus (E) (kN/m^2/m)	Poisson's Ratio (v)
Moorum fill	20	0	40	5	$100x10^3$	0.35
Softy marine silty clay	16	20	0	0	$87.1x10^3$	0.4
Medium stiff clay	17	50	0	0	$197.71x10^3$	0.45
Very stiff clay	19	112	0	0	$378.25x10^3$	0.45
Hard marine silty clay	20	200	0	0	$578.68x10^3$	0.4
Basalt rock	22	700	0	0	$1.25x10^6$	0.25

Numerical Modeling

Governing Factors

Numerical models involving FEM can offer several options/ alternatives to provide realistic solutions. The accuracy of these solutions depends on the modeler's ability to include the sequence of operations in the field. Often the problem being modeled is complex and simplifications have to be made to obtain a solution. Two of the governing factors which have a vast impact on both the real and model piles are; (1) the constitutive model used (2) the soil-structure interaction effect.

Constitutive Models

FEM has become popular as a soil response prediction tool. This has led to a higher demand for researchers to develop more comprehensive descriptions for soil behaviour, which in turn leads to more complex constitutive relationship. Prevost and Popescu (1996) state that for a constitutive model to be satisfactory it must be able to; (1) make a statement about the material behaviour for all stress and strain paths; (2) identify model parameters by means of standard material tests and (3) physically represent the material response to changes in applied stress or strain.

Previous studies have explored constitutive models and found that the use of isotropic models such as elastic, Mohr-Coulomb and Druker-Prager are sufficiently accurate (Chen and Saleeb, 1983). In the past linear elastic constitutive models have been commonly used in developing pile design methods (Poulos and Davis, 1990).

Plane Strain

Several forms of finite element analysis with various approximations have been proposed to assess the response of piles as influenced by lateral soil movements. The finite element approaches include three dimensional analysis, plane strain analysis and axisymmetric analysis. In this present study, plane strain finite element approach is adopted.

Randolph (1981) and Stewart et al. (1993) performed a site specific plane-strain analysis, where the piles were replaced by an equivalent sheet-pile wall with flexibility equal to the average of the piles and soil it replaced is shown in Figure 4. The sheet pile wall was modeled with stiffer elements within the finite element mesh. Springman (1984) continued analyses of this type with the embankment represented by the self-weight of linear elastic elements and the soft clay represented by either linear elastic or modified Cam-clay models. This form of analysis allows pile groups to be analysed directly by incorporating them into the finite element mesh, though single piles can be adequately represented, since the equivalent sheet-pile wall models a row of equally spaced piles.

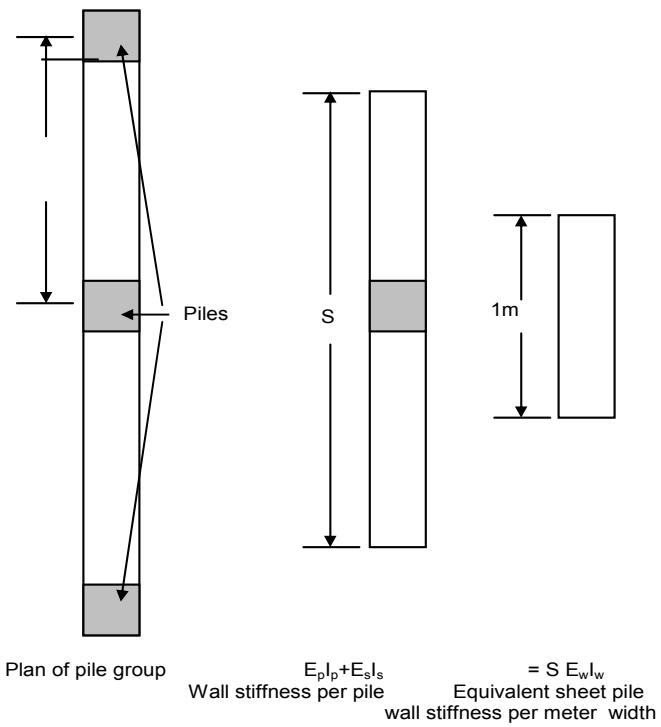

Fig. 4 Equivalent Sheet Pile Wall Representation of Piles for Plane Strain Finite Element Analysis

Naylor (1982) extended this type of approach by connecting the sheet-pile wall to the soil with link elements, thus allowing relative displacement of the soil and the wall, and more closely approximating the true three dimensional behaviour around the piles. However, limiting soil pressure between the soil and wall was not allowed for, since the soft stratum, embankment and link elements were represented by linear elastic models. The conclusions arising from that study were that link elements were not required in cases where the piles were quite flexible or the soft layer was deep. A similar approach was adopted by Rowe and Poulos (1979) for the analysis of stabilizing piles installed at the crest of a slope, although an elastic-plastic soil model was used and limiting soil pressure on the piles were specified to allow plastic flow of the soil past the piles.

Description of Approach

For this study, the berthing structure was analyzed using a plane strain finite element approach, with the piles represented as equivalent sheet- pile wall (Figure4). Plane strain analysis is the most straightforward of the finite element approaches described above, and allows good representation of the pile group configuration and geometry, without being unduly complicated. The equivalent sheet-pile walls are modeled with beam-column elements connected to the finite element mesh, and the soil strata are represented by 15 nodded triangular elements of elastic-plastic Mohr-Coulomb model. Soil-structure interaction (interface) is modeled by means of a bilinear Mohr-Coulomb model. The finite element program PLAXIS is used for this study.

In the model study, the same dimensions of the field berthing structure are adopted. To avoid the boundary effect in the numerical model, the boundary of stratigarphy of the model is taken as two times greater than the structural area. The soil strata are modeled with 15 noded triangular elements and the equivalent sheet-pile walls and pile cap are defined by five nodded beam-column elements with nodes separate from those defining the soil.

The soil nodes and pile nodes are connected by bilinear Mohr-Coulomb interface elements. This allows an approximate representation of the development of lateral resistance with relative soil-pile movement and ultimately the full limiting soil pressure acting on the piles. The stratigraphy is represented using finite elements and then their own self-weight loading is applied to the mesh to simulate in-situ stress condition.

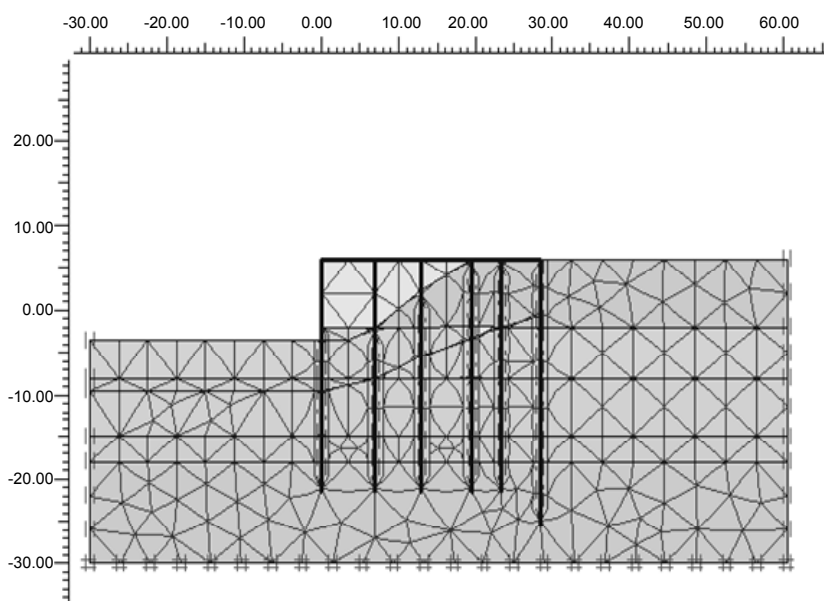

Fig. 5 Discretization of Finite Element Mesh (Fine Mesh)

The typical finite element discretization of the berth is shown in Fig 5. The soil stratum is idealized by 15 nodes triangular elements with elastic-plastic

Mohr Coloumb model and the structural elements are idealized by beam element. For the fine mesh FE discretization, the total number of elements is 427, nodes is 3905 and node stress points is 5124.

Material Parameters

Soil Properties

The analyses are conducted with moorum fill soil, soft to hard marine clay and basalt represented by Mohr-Coulomb model. The Mohr-Coulomb model is used for the proposed (linear elastic-plastic) model, with plastic flow governed by an associated flow rule. Value of angle of internal friction and dilatancy angle are input for the top layer of moorum fill soil. The values untrained shear strength with depths is input for each layer of elements for soft to basalt marine clay. These values (c, φ) are obtained from the laboratory tests (unconfined compressive test, direct shear test & triaxial test) conducted on selected soil samples collected at different depths. Young's modulus (E) profiles are estimated for each layer by using a relation between SPT (N) values and Young's modulus given by Mori (1964).

The values of Young's modulus at selected depths are also obtained by triaxial test and the obtained values are comparable with estimated values. Poisson's ratio values are appropriately selected for each layer. The values of soil properties are presented in Table-1. Initial stresses are generated for each clay layer of elements by appropriate density, which is also included in Table-1. Initial stress is generated in moorum fill layer by specifying a constant value of K_o = 0.4 (initial stress at rest condition, for $\varphi=40^o$). The excavation (dredging) is modeled by three equal excavation of each 2.12m in thickness.

Structural Properties

The piles, diaphragm wall and pile cap are represented by five noded beam-column elements. The beam elements are based on Mindlin's beam theory. This theory allows for beam deflection due to shearing as well as bending. In addition, the element can change length when an axial force is applied. Bending (flexural rigidity) stiffness EI and axial stiffness EA are input as the average of the soil and pile properties over an equivalent 1m thickness of the mesh. Thus the bending moments and shear forces resulting from the analysis are factored up by the pile spacing to obtain the bending moments and shear forces per pile. As the soil stiffness is much lower than the structural stiffness, the equivalent wall properties are effectively independent of the soil properties and do not vary with depth.

Table 2: Structural Member Properties (without Creep)

Description	Axial Modulus (EA) (kN/m)	Rigidity Modulus (EI) (kN/m^2/m)	Poisson's Ratio (v)	Equivalent Thickness (t)(m)
Pile	4.552×10^7	5.57×10^6	0.15	1.212
Pile cap	1.775×10^7	5.324×10^5	0.15	0.6
Diaphragm wall	3.253×10^7	3.28×10^6	0.15	1.1

The structural member's properties are presented in Table-2. In order to consider the effect of creep on concrete in the model study, the Young's modulus of concrete is calculated by using the equation given in Bureau of Indian Standards - 456 (2000).

$$E_{sc} = E_s / (1+\varphi_c) \quad (1)$$

The value of φ_c is taken as 1.6 for after 28 days of the berth construction. The structural element properties including creep effect is given in Table.3

Table 3: Structural Member Properties (with Creep)

Description	Axial Modulus (EA) (kN/m)	Rigidity Modulus (EI) (kN/m^2/m)	Poisson's Ratio v	Equivalent Thickness (t) (m)
Pile	1.75×10^7	2.13×10^6	0.15	1.211
Pile cap	6.82×10^6	2.05×10^5	0.15	0.6
Diaphragm wall	1.25×10^7	1.26×10^6	0.15	1.099

Soil-Structure Interface

Fifteen noded soil elements and five noded structural elements are connected with 5 pairs of interface elements as show in Figure 6. In the figures the interface elements are shown to have a finite thickness, but in the finite element formation the coordinates of each node pair are identical, which means that the element has a zero thickness. Each interface has assigned to it a Virtual thickness which is an imaginary dimension used to obtain the material properties of the interface. The Virtual thickness is defined as the virtual thickness factor times the average element size. The value of Virtual thickness factor is 0.1. The average element size is determined by the global coarseness for the mesh generation. The stiffness matrix for interface element is obtained using Newton-Cotes integration points. The position of these integration points (or stress points) coincides with the position of the node pairs.

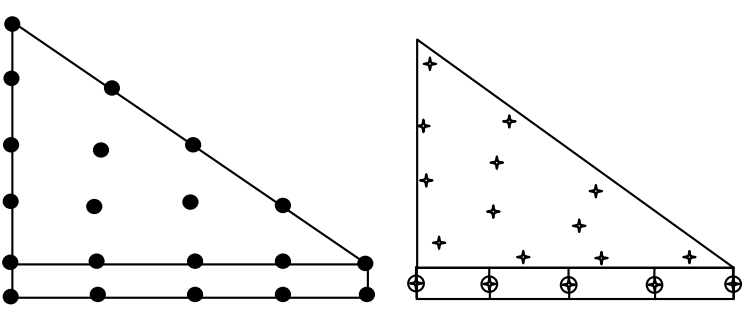

(a) Nodes (b) Stress points

Fig. 6 Distribution of Nodes and Stress Points in Interface Elements and Connection with Soil Element

Results and Discussion

After construction of the full berth, the inclinometer readings are taken in 3 stages. First readings are taken after construction of the berth and before starting dredging. These represent the initial position of the diaphragm wall and pile. The second readings are taken immediately after dredging up to -9.5m depth. The difference between second readings and first readings are the deflected shape of the diaphragm wall panel and pile. The third readings are taken after 3 months of -9.5m dredging. The difference between third and second readings is the further deflected shape of the diaphragm wall and pile, which is due to structural and soil creep. The field test results are compared with FEM results.

Figure 7 shows the deformed mesh of the berthing structure after -9.5m dredging. It is observed that the soil movement is much greater in top layers of moorum fill and soft marine clay. From the deformed shape of the mesh, it can be observed that the failure zone is like a slip circular failure and the critical slip circle may pass through the soft marine clay layer.

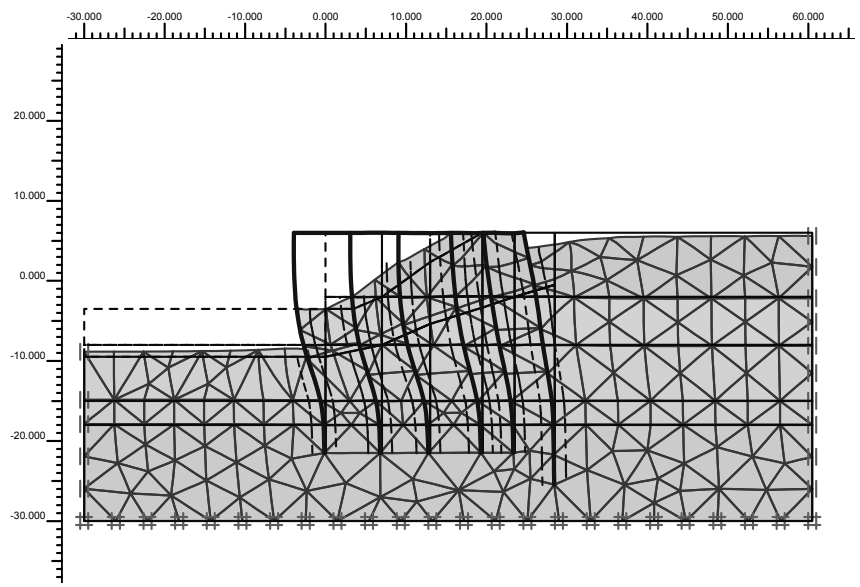

Fig. 7 Deformed Mesh (Displacement Scaled upto 200 times)

Initially the analysis is carried out for different types of mesh in order to check the convergence of the mesh size. Four different types of mesh (coarse, medium, fine and very fine) have been taken for this analysis. The comparison of deflection for different meshes is shown in Figure 8. It is observed that there are no significant changes in the deflection by changing the mesh size; all four meshes are showing almost the same deflection. Figure 9 and 10 shows the deflection comparison of both 6 node element and 15 node element of diaphragm wall and pile respectively. The 15 node element give good agreement with field results than 6 node elements and hence the entire analysis is done by 15 node triangular element with fine mesh.

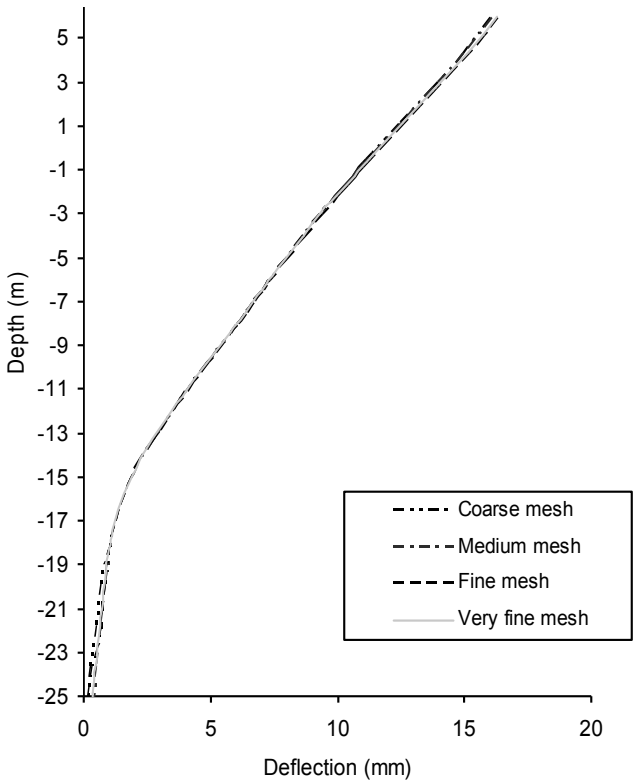

Fig. 8 Convergence of Different Meshes

From the full scale model tests, immediately after -9.5m dredging level, the maximum deflection of 15.2mm and 20.3mm is observed for diaphragm wall and pile respectively. The FEM result is in good agreement with field result obtained just after dredging (-9.5m dredge level) without considering the creep effect.

Figure 11 and 12 shows the deflection comparison of both full scale field test results and FEM results of after 3 months of -9.5m dredging of diaphragm wall and pile respectively. The maximum deflection of 17.3mm and 22.8mm is observed for diaphragm wall and pile respectively. The increase in deflection may be due to creep behaviour of concrete and clay soil. In the FE analysis, the concrete creep is taken in to account by considering reduced stiffness values (equation-1). The FEM results are observed to underestimate the deflection by 15% in diaphragm wall when compared with field test only in the layers of soft marine clay and medium stiff clay, which may be due to the effect of creep of clay layers. In the present FEM model, the soil creep effect is not considered. However, pile deflection is not much significant even though without considering the creep effect of clay layers.

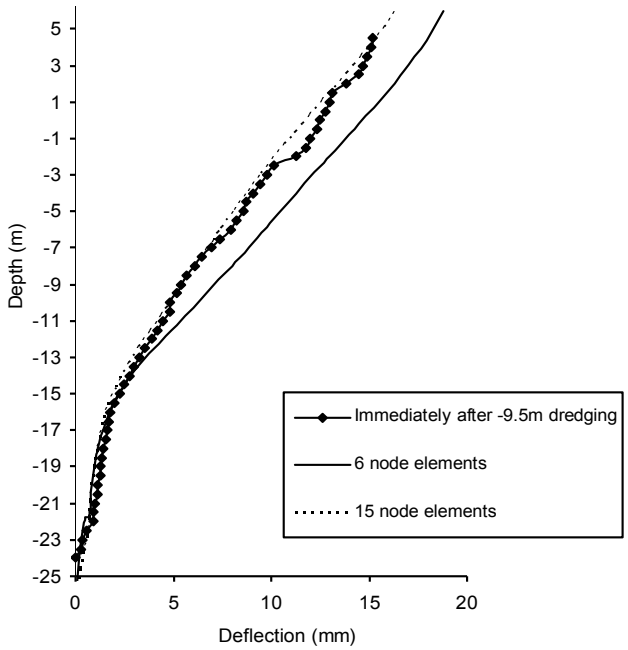

Fig. 9 Comparison of Measured Deflection with FEM Result for Diaphragm Wall (without Creep Effect)

Figure 13 shows the typical bending moment variation of diaphragm wall of with and without creep effect. The maximum bending moment is observed at a depth of 12d from ground surface for both cases, where the hard marine silty clay stratum is starting. The bending moment variation is more for without considering creep effect than with creep effect, which may be due to reduction of rigidity modulus of structural members while considering the concrete creep effect. The maximum bending moment is reduced by 30% while considering the effect of creep on concrete.

Variation of shear force in diaphragm wall is presented in Figure 14, which includes concrete creep effect. The maximum shear force is observed at a depth of 10.5d, where the soil strata changing from stiff clay to hard marine silty clay. The influence of creep is not much significant in the maximum shear force. However, there is significant reduction in shear force at the top layers, which may be due to increasing relative stiffness of the bottom layers (hard strata).

Bending moment and shear force variation of pile is presented in Figure 15 and 16 respectively. The maximum bending moment is observed at a depth of 12d and maximum shear force is observed at a depth of 10.5d. The maximum bending moment is reduced by 33% and the maximum shear force is reduced by 25% while considering the effect of creep on concrete. However, the shear force variation at the top layers is not much significant, which may be due to reduction of passive resistance mobilized in front of pile. The shear force variation is almost constant from depth +6m to -6m where the influence of dredging is much significant.

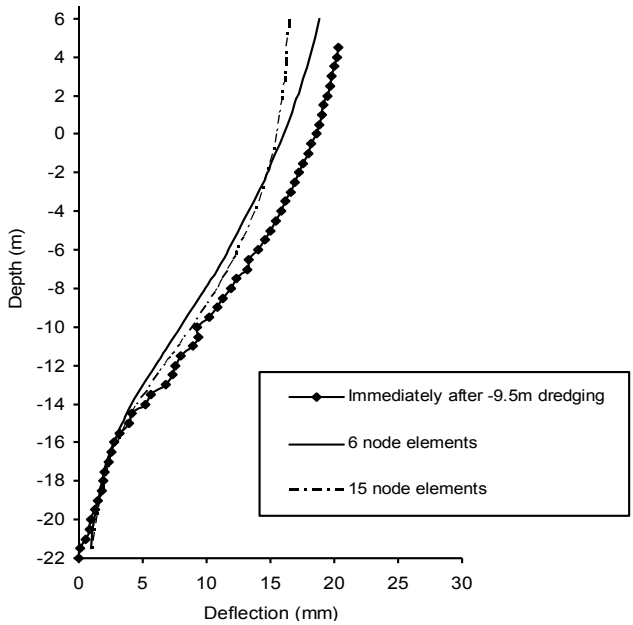

Fig. 10 Comparison of Measured Deflection with FEM Result for Pile (without Creep Effect)

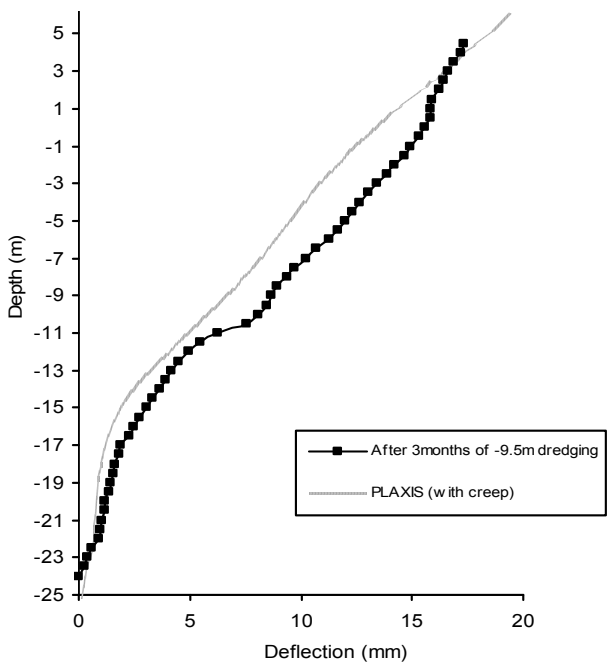

Fig. 11 Comparison of Measured Deflection with FEM Result for Diaphragm wall (with Creep Effect)

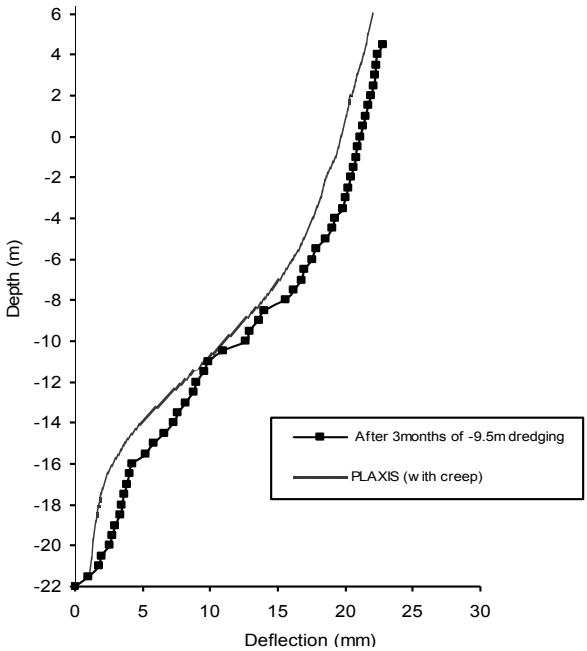

Fig. 12 Comparison of Measured Deflection with FEM Result for pile (with Creep Effect)

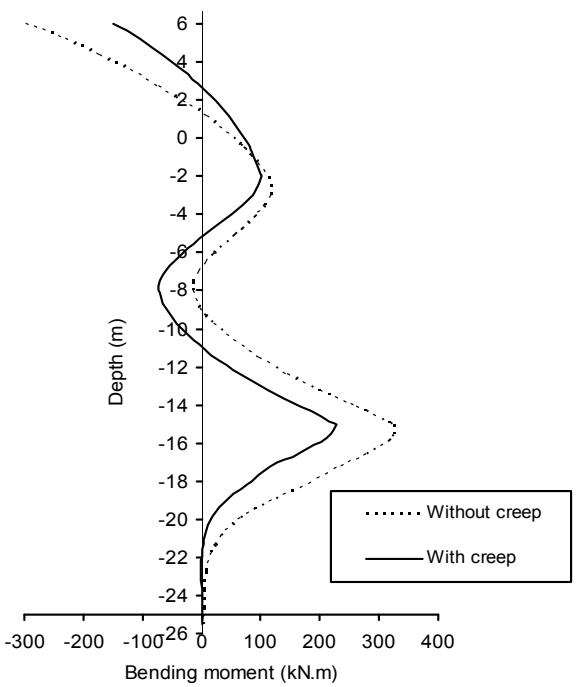

Fig. 13 Typical Bending Moment Variation in Diaphragm Wall

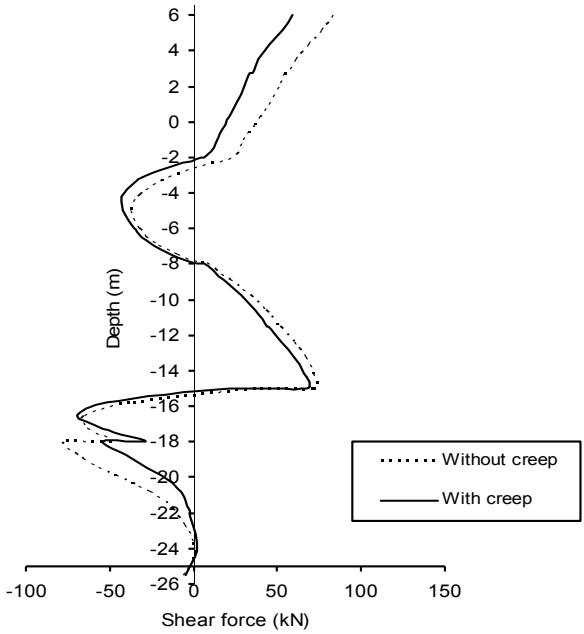

Fig. 14 Typical Shear Force Variation in Diaphragm

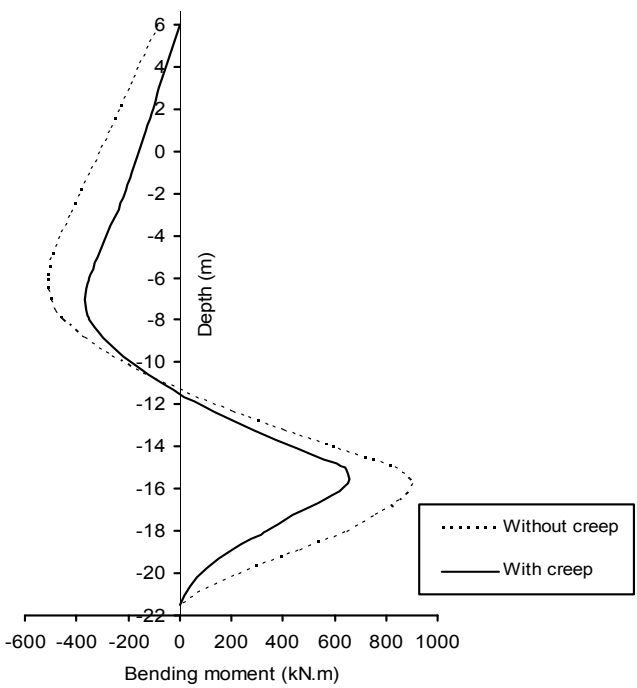

Fig. 15 Typical Bending Moment Variation in Pile

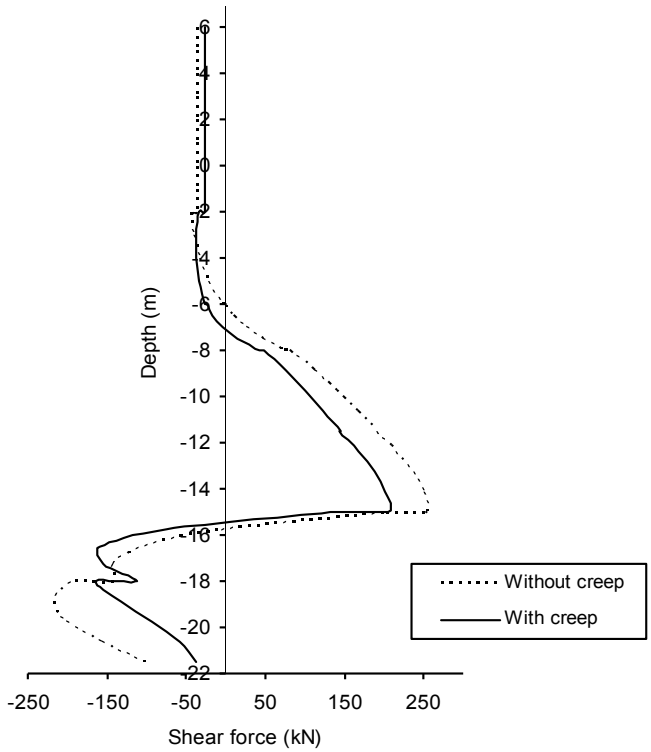

Fig. 16 Typical Shear Force Variation in Pile

Conclusions

The paper describes the numerical study examining the response of diaphragm wall and pile supported berthing structure during dredging. The numerical model results are compared with field test results.

Plane strain finite element analysis was used in which piles were represented by equivalent sheet-pile wall. Mohr Coloumb model was used to model the soil stratum. The FEM results compared well with full scale field measurements and generally yielded acceptable bending moments and deflections over a dredged depth of -9.5m level was affected by the relative soil-structure stiffness.

Creep effect of concrete was investigated using reduced structural stiffness. However, in the present study the effect of soil creep is not included. If the soil creep is included, the comparison between finite element results and the full scale field data would be significantly better.

Based on this work, it may be concluded that the developed numerical model (plane strain analysis) using PLAXIS compares well with full scale field data.

List of Symbols and Abbreviation

c_u - Cohesion (FL^{-2})
d - Pile diameter (L)
E_s - Young's modulus of concrete (FL^{-2})
E_{sc} - Young's modulus of concrete after considering creep (FL^{-2})
EA - Axial modulus (F)
E_sI_s - Rigidity modulus of soil (FL^2)
E_pI_p - Rigidity modulus of pile (FL^2)
E_wI_w - Total rigidity modulus of both soil and pile (FL^2)
K_o - Coefficient of earth pressure at rest condition (dimensionless)
N - Standard penetration test value (dimensionless)
S - Spacing between piles (L)
t - Equivalents thickness (L)
φ - Angle of internal frication (degrees)
φ_c - Creep coefficient (dimensionless)
ψ - Dilatancy angle (degrees)
v - Poisson ratio (dimensionless)
γ_{sat} - Saturated unit weight of soil (FL^{-3})
γ_{sub} - Submerged unit weight of soil (FL^{-3})

References

Bureau of Indian Standards-*456 (2000) Plain and reinforced concrete code of practice*, New Delhi.

Chen, W., and Saleeb, A. (1983) *"Constitutive Equations for Engineering"*, Fourth ed. PWS Publishing, Melbourne.

Chen, S. F., and Yap, T. F. (1991) "Effect of construction of a diaphragm wall very close to a masonry building", *Proc., Symp. Slurry Wall: Des. Constr. and Quality Control*. ASTM Spec. Tech. Publ., West Conshohocken, 1129, pp 128-139.

Clough, G.W., and O'Rourke, T. D. (1990) "Construction induced movements of in-situ wall", *Proc., Des. and Perf. of Earth Retaining Structure Geotech*. Spec. Publ. No. 25. P.C. Lambe and L. A. Hansen, eds., ASCE, New York, pp 439-470.

Davies, R.V. (1982) "Special considerations associated with constructing diaphragm walls in marine deposits and residual soils in Southeast Asia", *Proc. Conf. on Diaphragm Walling Techniques*, CI-Premier, Singapore, RDS1-12.

Dibiagio, E., and Myrvoll, F. (1972) "Full scale field tests of a slurry trench excavation in soft clay", *Proc., 5th Eur. Conf. on Soil Mech. and Found. Engg*., Spanish Society for Soil Mechanics and Foundations. Spain, I, pp 1461-471.

Mori, H. (1964) "The behaviour of steel pipe piles under vertical and horizontal loads", *Proceedings of Symposium on Bearing capacity of piles*, Roorkee, India, 106-115.

Naylor, D.J. (1982) "*Finite element study of embankment loading on piles*", Report for the Department of Transport, Department of Civil Engineering, University College of Swansea.

Poh, T. Y., Goh, T. C., and Wong, I. H. (2001) "Ground movements associated with wall construction: case histories", *Journal of geotechnical and Geoenvironmental Engineering*, ASCE, 127(12), pp 1061-1069.

Poulos, H.G., and Davis, E.H. (1990) "*Pile foundation analysis and design*", John Wiley & Sons, Inc, Toronto.

Prevost, J.H., and Popescu, R. (1996) "Constitutive relations for soil materials", *Electronic Journal of geotechnical Engineering*.
http://www.ejge.com/1996/Ppr9609/Ppr9609.htm

Randolph, M.F. (1981) "*Pilot study of lateral loading of piles due to movement caused by embankment loading*", Report for the Department of Transport, Cambridge University.

Rowe, R.K., and Poulos, H.G. (1979) "A method for predicting the effect of piles on slope behaviour", *3rd ICONMIG*, Aachen, Vol. 3, pp 1073-1085.

Springman, S.M. (1984) Lateral loading on piles due to embankment construction, *M. Phil. Thesis,* Cambridge University.

Steward, D.P., Jewell, R.J., and Randolph M.F. (1993) "Numerical modeling of piled bridge abutments on soft ground", *Computers and Geotechnics*, Vol 15, pp. 23-46.

Tamano, T., Fukui, S., Suzuki, H., and Ueshita, K. (1996) "Stability of slurry trench excavation in soft clay", *Soils and Foundation*, Tokyo, 36(2), pp 101-110.

Tedd, P., Chard, B. M., Charles, J. A., and Symonds, I. F. (1984) "Behaviour of a propped embedded retaining wall in stiff clay at bell common tunnel", *Geotechnique*, London, 34(4), pp 513-532.